

PAPER • OPEN ACCESS

Multi-facility comparison of InGaAs trap detector responsivity for optical fiber power

To cite this article: Kyle Rogers *et al* 2025 *Metrologia* **62** 045010

View the [article online](#) for updates and enhancements.

You may also like

- [In Situ Measurement of Oxygen Partial Pressure in a Cathode Catalyst Layer](#)
William Epting, Katherine C. Hess and Shawn Litster
- [Quantitative characterization of surface topography using spectral analysis](#)
Tevis D B Jacobs, Till Junge and Lars Pastewka
- [\(Invited\) Cell Performance Analysis of Redox Flow Fuel Cells with Pt-Free Cathode](#)
Tatsuya Hatanaka, Kenji Kudo, Takamasa Nonaka et al.

Multi-facility comparison of InGaAs trap detector responsivity for optical fiber power

Kyle Rogers^{1,*} , Jeanne Houston² , Zeus Ruiz³, Matthew Spidell¹ , Padraic Aither¹ , Marty Gould⁴ and John Lehman¹ 

¹ National Institute of Standards and Technology, Applied Physics Division, 325 Broadway, Boulder, CO 80305, United States of America

² National Institute of Standards and Technology, Sensor Science Division, 100 Bureau Drive, Gaithersburg, MD 20899, United States of America

³ Centro Nacional de Metrología, Querétaro, Mexico

⁴ Zen Machine & Scientific Instruments, 1568 Steamboat Valley Rd, Lyons, CO 80540, United States of America

E-mail: kyle.rogers@nist.gov

Received 10 June 2025, revised 14 August 2025

Accepted for publication 21 August 2025

Published 1 September 2025



CrossMark

Abstract

The absolute responsivity of an optical detector in a trap configuration has been investigated in the interest of high-accuracy fiber-coupled measurements for commercial optical fiber power meters and fiber-coupled single-photon detector calibrations. The highest accuracy measurements of optical power are typically undertaken free space and then disseminated for fiber-coupled measurements with some additional uncertainty. At the lowest uncertainty, the difference between free-space and fiber-coupled optical power measurements can be significant. We present here a complete evaluation of multiple trap detectors consisting of two InGaAs photodiodes and a concave mirror. This evaluation includes fiber-based responsivity at discrete laser wavelengths measured both with cryogenic and room temperature standards (diverging input beam), free-space absolute spectral responsivity over a broad wavelength range (converging beam), free-space responsivity at discrete laser wavelengths (collimated), linearity, and spatial uniformity.

Keywords: trap detector, fiber optic power meter, laser power calibration

1. Introduction

Future quantum communication networks are likely to be undertaken with the very practical implementation of sources and detectors coupled through optical fiber [1]. In the ideal world of secure quantum communications, the use of detectors

having very high quantum efficiency requires accounting for every photon in the network to maintain the quantum nature of the measurement. A low-efficiency detector will produce high inequivalence with a quantum detector, especially in the low-pW regime where measurements take place. The exploitation of sophisticated fiber-based detectors that are photon-number resolving and counting faces a very real-world challenge of losses due to poor splices, mechanical fiber connectors, and poor coupling efficiency [2]. Such losses are typically measured as a change in optical power as the light propagates through these splices, connectors, and other components. To work in characterizing performance in the quantum regime, the uncertainty on these measurements must be very low. Traditional fiber calibration systems provide

* Author to whom any correspondence should be addressed.



Original content from this work may be used under the terms of the [Creative Commons Attribution 4.0 licence](https://creativecommons.org/licenses/by/4.0/). Any further distribution of this work must maintain attribution to the author(s) and the title of the work, journal citation and DOI.

higher uncertainties [3] than free-space systems that can operate at lower power levels [4]. In this work, we ask the very simple question: How do we compare optical power measurements made with free-space beams to those made with fiber coupled beams? In the early days of optical fiber power measurements, the fiber connector to a detector was simple and the results variable. Early improvements were made by adding an anti-reflection or absorptive coating to the adapter cap holding the fiber connector and facing the detector under test [5]. While useful because they reduce scattered light, such improvements do not fully account for the offset or additional uncertainty attributable to the differences between fiber and free space. To improve the accuracy and reproducibility of optical fiber power measurements, we developed a variation on the ‘trap detector’ by replacing a diode in the trap with a retroreflecting concave mirror [6]. The mirror compensated for losses from light diverging from the end of a fiber and provided a basis for rigorously defining the coupling efficiency from the fiber tip into the trap detector. The trap detector design is nearly twenty years old, but the significance of the problem it addresses is undiminished as we seek to improve the fiber-based calibration of quantum detectors.

The detector packaging and design is similar to that described by Lehman and others [6, 7] using Ge and Si photodiodes. For this manuscript, we will refer to these as ‘fiber traps.’ The fiber traps discussed here are constructed with two $\varnothing 10$ mm InGaAs (IGA) photodiodes followed by a concave mirror. IGA was chosen over a Ge-photodiode design due to higher quantum efficiency and reduced ambient temperature variation effects (eliminating the need for temperature control which simplifies the assembly). The two-diode design is an evolved geometry from even earlier three-diode trap designs for achieving high external quantum efficiency [8]. The fiber trap has high external quantum efficiency (99.9%), but it is optimized for equally high coupling efficiency for collimated, converging (up to $f/4$), and diverging (numerical apertures up to 0.24) input from an optical fiber connector (single mode fiber up to 1750 nm) [7]. To achieve this high coupling efficiency, the diode spacing and arrangement requires a custom ‘home plate’ shaped diode carrier with minimal margin between diodes. A photo and layout of the diode arrangement is shown in figure 1. Figure 1(a) illustrates the IGA diodes mounted on the custom carrier, providing the maximized coupling efficiency. Figure 1(b) shows the propagation of diverging rays from a fiber input end through the trap. From the input, light is incident on the first diode, then the second diode, then the concave mirror. The mirror then reflects any remaining light back through the two diodes, allowing for very high efficiency. The distance from the end of the fiber output to the mirror is 25 mm. The input aperture to the detector is a threaded disk that further limits the aperture to $\varnothing 7.1$ mm for free space measurements (although the input beam is typically much smaller). For the fiber-based measurements, a fiber adapter cap is threaded into the input. This adapter cap is painted with a carbon nanotube-doped paint to minimize scattered and back-reflected light [9].

The mirror used is a $\varnothing 15$ mm, 40 mm focal length, plano-concave mirror with an ‘enhanced silver’ coating on the

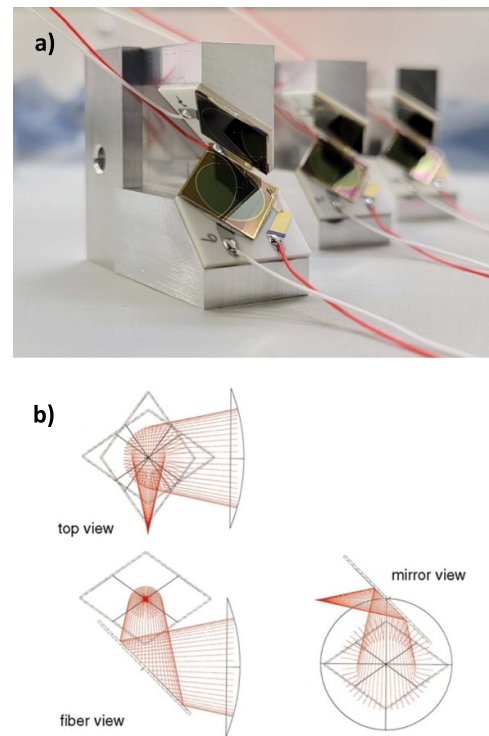


Figure 1. Pictures of (a) fiber traps without the mirror and (b) schematic view of the diodes including the mirror. Reproduced with permission from [6]. © Optica Publishing Group.

concave side. The focal plane of the light reflected from the mirror occurs between the two diodes, such that the light is diverging as it exits the trap. For this work, eight identically constructed IGA trap detectors were compared across laboratories with differing beam input conditions. Each laboratory performed a calibration of each detector using their respective procedures at a nominal wavelength of 1550 nm. Additionally, one detector was characterized for both spatial uniformity and linearity.

2. Relative characterization

2.1. Spatial uniformity

During the free-space calibration using the monochromator-based NIST visible to near-infrared spectral comparator facility (Vis/NIR SCF) [10], the spatial uniformity of each fiber trap was evaluated. Evaluation of the spatial uniformity of the detector is essential given the input beam characteristics are different for each laboratory (converging, diverging, and collimated). Each detector was mounted such that automated control of both the horizontal and vertical axis (with respect to the aperture plane) was performed using the control software. The Vis/NIR SCF has an automated protocol for aligning the test detector for spectral responsivity calibration, which determines the center of the detector using 80% falloff in signal at points across the horizontal and vertical directions. This centering procedure is repeatable to 0.1 mm, even for non-uniform detectors. A version of this centering procedure is used for the

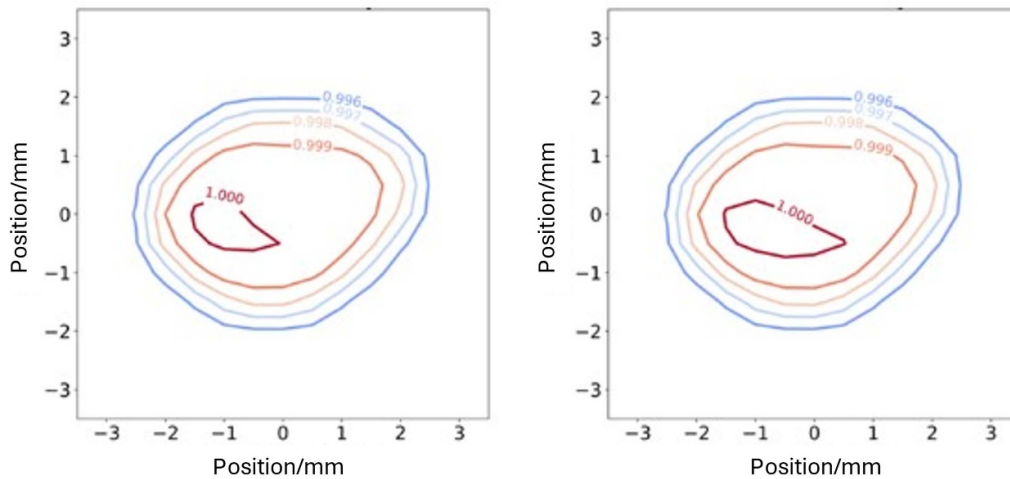


Figure 2. Spatial uniformity scans for an InGaAs fiber trap at 1300 nm (left) and 1550 nm (right).

spatial uniformity scan that acquires relative responsivity to a peak value across the detector area. For the data presented here, a nominal 6 mm by 6 mm scan area with a 0.5 mm step size and 1 mm by 1 mm beam was used (focused at the mirror element). Figure 2 illustrates the spatial uniformity scans for a typical fiber trap (all traps exhibited uniformity within the presented 0.4%, so these results are typical) at both 1300 nm and 1550 nm. Each contour represents a 0.1% change in responsivity, showing the sampled detector is nearly uniform across the entirety of input aperture.

2.2. Linearity

Typical optical fiber detectors allow for measurement across a large dynamic range but may experience non-linearity at certain power levels and particularly near power levels near decadal range changes (sometimes called range discontinuities). An understanding of power-dependent responsivity is imperative for single-photon detection systems [11]. Linearity of the fiber trap detectors was assessed using a fiber-based linearity system that relies on the triplet-superposition method [12]. Given the geometry of all detectors is identical and the diodes used in each trap are from the same two wafers (one diode from each wafer), the linearity for all traps illustrated a similar behavior. The typical noise floor of the fiber traps is 0.1 nW, which determined the linearity scan lower limit. The linearity was assessed from attenuation levels of 0 dB to 59 dB, corresponding to roughly the power range of 2 nW–2 mW. The correction factor (CF) produced by the linearity measurements relates an absolute power calibration (in this case performed at nominally 100 μ W, or around 12 dB) to any power over the entire dynamic range of the trap. Thus, the CF for each power level is multiplied by the absolute power calibration factor to obtain the calibrated result. The trap reading is then divided by this product of factors to produce the calibrated value. Table 1 shows linearity results for one fiber trap and the expanded uncertainty of the CF at $k = 2$.

3. Free-space input characterization

3.1. Spectral responsivity (converging beam): VIS/NIR SCF

The spectral radiant power responsivity of each of the eight fiber traps was determined from 700 nm to 1800 nm in 5 nm increments by comparisons to temperature-controlled IGA photodiode working standards (WS), IGA-WS #1 and IGA-WS #3, using the monochromator-based NIST Vis/NIR SCF. The Vis/NIR SCF operates nearly identically to the visible spectral comparator facility described by Houston *et al* [10]. The spectral comparisons between the test fiber trap detectors and working standard photodiodes were performed using a double monochromator illuminated by a tungsten quartz-halogen lamp as a tunable monochromatic source. The aperture of the Vis/NIR SCF monochromator was imaged ($\approx f/9$) on the test fiber trap's aperture and the trap detector was moved forward 25 mm in the optical path resulting in a 1.0 mm² beam on its internal mirror. Each fiber trap was angularly aligned to the optical path using a microscope slide secured parallel to the input aperture (flush against its case). The beam was centered on- and underfilled the photosensitive area.

The wavelength scale of the monochromator was calibrated with laser and emission lines to within an uncertainty of ± 0.1 nm over the entire spectral range. The full-width half-maximum bandpass of the monochromator was 4 nm. The short-circuit photocurrents from the test fiber trap and each working standard photodiode were measured with calibrated transimpedance amplifiers. Beam power fluctuations were monitored with a beamsplitter and an additional temperature-stabilized IGA trap. The spectral radiant power responsivity scale is based on the NIST reference absolute cryogenic radiometer [4]. The spectral radiant power responsivity of one test fiber trap detector listed in A/W at each wavelength is plotted in figure 3. The uncertainty in the NIST spectral radiant power responsivity scale is described in [10]. The relative expanded uncertainty ($k = 2$) for this measurement is also plotted in figure 3 at each wavelength. The increase in uncertainty between 1300 nm and 1500 nm is due to a water absorption

Table 1. Linearity results for fiber trap.

Nominal Attenuation/dB	Nominal input power	CF	Expanded uncertainty ($k = 2$, 95% confidence)
0	2 mW	1.0000	0.10%
5	0.5 mW	1.0000	0.10%
10	0.15 mW	1.0000	0.10%
12	100 μ W	1.0000	0.10%
20	15 μ W	1.0000	0.10%
25	5 μ W	1.0001	0.10%
30	1.5 μ W	1.0001	0.10%
35	0.5 μ W	1.0002	0.10%
40	0.15 μ W	1.0007	0.10%
45	50 nW	1.0021	0.10%
50	15 nW	1.0070	0.11%
55	5 nW	1.0200	0.15%
59	2 nW	1.0508	0.30%

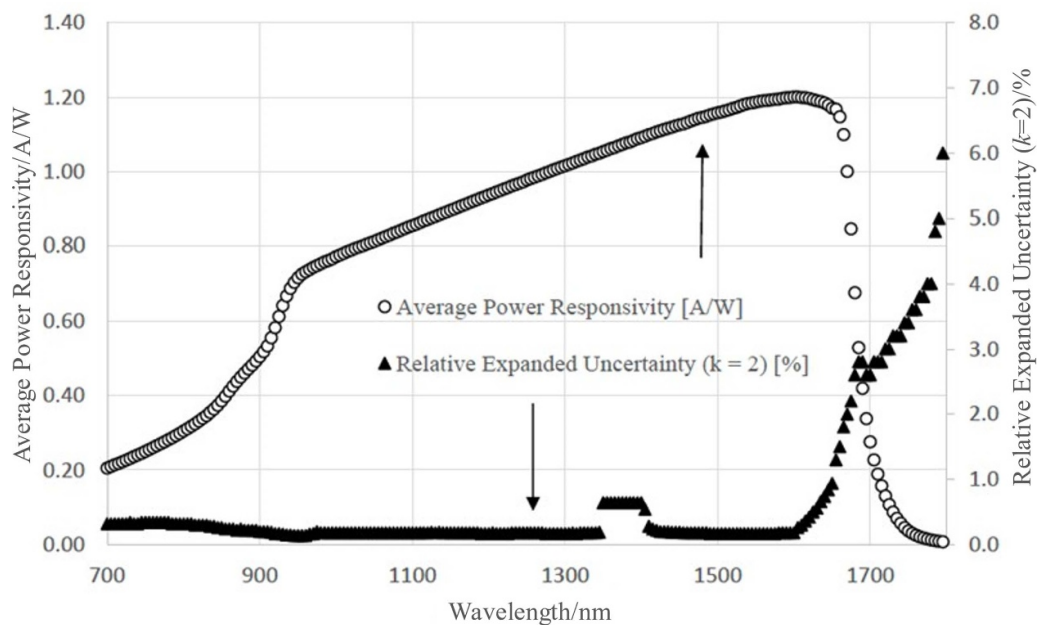


Figure 3. Spectral responsivity calibration results for one fiber trap detector. The left axis describes the average responsivity (plotted in circles) while the right axis describes expanded uncertainty (plotted in triangles), both with respect to wavelength. These results are typical for all the detectors measured in this work.

band in the transfer standard calibration that slightly increases the noise of the measurements. The power responsivity of all eight fiber traps at a wavelength of 1550 nm is shown in table 2, and the expanded uncertainty given in table 3.

3.2. Absolute responsivity (collimated beam): C-lab

Comparisons for each of the eight fiber traps were made in the precision free-space continuous wavelength laboratory (referred to here as ‘C-lab’) using a room-temperature radiometer primary standard known as the NIST planar absolute radiometer for room temperature (PARRoT) [13]. The laser beam had a vacuum wavelength of 1549.727 nm (diode laser) and a spatial profile maximum extent of 2 mm. The vacuum wavelength is the weighted average of the spectral

power density assessed by an optical spectrum analyzer and is traceable to the SI by way of a 1523.488 nm He-Ne laser which serves as an intrinsic wavelength standard with wavelength relative standard uncertainty of 0.00015% [14]. An uncertainty contribution for the optical spectrum analyzer was not assessed. A precision picoammeter was used as the effective meter to output each detector’s current.

Each fiber trap’s entrance aperture was centered and normal to the incident beam. A beam splitter ratio was determined by concurrently measuring the power incident on the standard and a monitor detector, used to detect any power fluctuations or other system instabilities. The power impinging upon each trap was then measured concurrently with the monitor detector. The beamsplitter ratio was measured again after the trap measurements. With the average beamsplitter ratio and

Table 2. Absolute responsivity results at nominally 1550 nm wavelength and 100 μ W.

NIST ID	Trap #	(1) Vis/NIR SCF /A/W	(2) OFPM /A/W	(3) C-lab/A/W	Max difference (1)–(3) /%
686 276	1	1.1397	1.1392	1.1388	0.08
686 277	2	1.1875	1.1869	1.1869	0.05
686 278	3	1.1869	1.1861	1.1862	0.06
686 279	4	1.1840	1.1805	1.1799	0.35
686 280	5	1.1405	1.1422	1.1421	0.15
686 281	6	1.1884	1.1877	1.1876	0.07
686 282	7	1.1405	1.1404	1.1397	0.07
686 283	8	1.1378	1.1404	1.1393	0.23

Table 3. Comparison of results across four labs at nominally 1550 nm and 100 μ W.

Trap #	NIST ID	Laboratory	Input beam condition	Responsivity /A/W	Expanded uncertainty ($k = 2$, 95% confidence)
1	686 276	Vis/NIR SCF	Converging	1.1397	0.17%
		OFPM	Diverging	1.1392	0.41%
		C-lab	Collimated	1.1388	0.15%
		OFCR	Diverging	1.1388	0.21%

monitor's power measurement, the power incident on the trap was inferred. The calibration factor was found by dividing the picoammeter reading used to acquire the output current by the calculated incident power. The results of this calibration are also summarized in table 2, and the expanded uncertainty given in table 3. A detailed uncertainty breakdown for the PARRoT is contained in [13].

4. Fiber-coupled input characterization

4.1. Optical fiber power meter calibration (diverging beam): (OFPM)

Each of the trap detectors were calibrated in a fiber-based system as an OFPM at a wavelength of 1549.6 nm (with a 0.13 nm standard uncertainty for each center wavelength based on refractive index in vacuum) by comparing them to a calibrated secondary standard. This secondary standard was an electrically calibrated pyroelectric radiometer (ECPR) which had previously been calibrated against the PARRoT (in the C-lab facility), which is in turn traceable to the SI through NIST representations of the Volt and Ohm [3, 13, 15]. The ECPR is a spectrally flat pyroelectric detector with a custom adapter cap that adequately fills the detector area with a diverging beam exiting the optical fiber. A fiber beam splitter ratio was determined by concurrently measuring the average power incident on the secondary standard and a photodiode monitor detector. This monitor detector also captures any power variations or other instabilities of the system, similar to that used in C-lab. The optical fiber was then moved to each fiber trap detector and the average power impinging upon the trap was measured concurrently with the monitor. With the beam splitter ratio and monitor's average power measurement, the average power incident on each trap was inferred. The single-mode fiber cable with an FC/PC connector (at the detector) used in

the measurements was constant across all the fiber trap detectors. Each trap was again used with a picoammeter as the effective meter.

Each fiber trap calibration factor was obtained by dividing its net display reading, recorded by the picoammeter, by the incident power. The results of this calibration are also summarized in table 2, and the expanded uncertainty given in table 3. A detailed uncertainty breakdown is contained in [3].

4.2. Optical fiber cryogenic radiometer calibration (diverging beam): (OFCR)

The NIST OFCR was used to calibrate one of the fiber traps at a wavelength of 1549.43 nm. The primary standard inside of the OFCR is a compact, microfabricated planar electrical substitution radiometer which features vertically aligned carbon nanotubes as an absorber [16]. The detector is 5.5 mm in diameter with the fiber ferrule positioned approximately 2 mm above the surface, which is an identical beam delivery case to the OFPM (diverging beam). The measurement setup for this calibration is identical to that described in [17]. Each channel of the Fabry–Pérot laser diode source was connected to a custom variable optical attenuator and shutter. The emitted laser light was then directed through a 2×1 optical switch to a paddle polarization controller, which optimized the angle and degree of polarization. Additional optical switches facilitated the routing of the signal to the standard, the fiber trap detector, or a polarimeter for monitoring and correcting any polarization drift. To ensure the integrity of the polarization state throughout the entire setup, polarization-maintaining fiber was employed from the laser to the detector. Prior to each measurement, all optical switches were characterized for their switching ratio stability, achieving stability levels of 0.046% for 1549.43 nm. The expanded uncertainty for the OFCR is given in table 3. A detailed uncertainty breakdown is contained in [17].

Table 4. Chi-squared values and consistency check.

Trap #	NIST ID	χ^2_{obs}	$\chi^2_{0.05}$	Consistency
1	686 276	0.5650	5.991	Satisfied

Table 5. DoE between four laboratories for INGAAT-1 detector.

Laboratories compared	DoE	Expanded uncertainty of DoE ($k = 2$, 95% confidence)
Vis/NIR-SCF vs OFCR	0.079%	0.27%
PARRoT vs OFCR	0.000%	0.26%
PARRoT vs OFPM	-0.035%	0.44%
Vis/NIR-SCF vs OFPM	0.044%	0.44%
Vis/NIR-SCF vs PARRoT	0.079%	0.23%
OFPM vs OFCR	0.035%	0.46%
Average	0.034%	0.35%

5. Results compared

5.1. All fiber traps across three labs

All eight fiber trap detectors were measured at 1550 nm (nominal) in three different laboratories (Vis/NIR SCF, OFPM, C-lab) at a nominal power of 100 μW . Each fiber trap is serialized as INGAAT-#, where # is the trap #. The results in table 2 below indicate responsivity values, presented as A/W, measured by each lab. The difference (column 6, table 2) indicates the maximum discrepancy between any two labs. The average max difference of 0.13% is significantly lower than that presented in 1999 by Lehman and Li, likely attributed to improved measurement capability (specifically in the converging beam case, the Vis/NIR SCF) [6]. The results for max difference are comparable to the $k = 2$ uncertainties of the individual labs (shown in table 3), indicating good agreement between the measurements.

5.2. INGAAT-1 across four labs

To further evaluate the equivalence of results, one fiber trap (INGAAT-1, NIST ID 686276) was calibrated against four laboratories (including the OFCR). An additional comparison of responsivity values is shown below in table 3 to include these results, as well as the expanded uncertainty associated with each lab.

The degree of equivalence (DoE) between each lab was assessed using the method set forth by the International Committee for Weights and Measures and the Consultative Committee for Photometry and Radiometry [18]. The Vis/NIR SCF laboratory was chosen for the pilot laboratory for the evaluation given its low uncertainty and very high measurement repeatability. Both a Chi-squared consistency check and bilateral DoE calculation were performed. For the Chi-squared check, both the observed (χ^2_{obs}) and standard ($\chi^2_{0.05}$) values were obtained in the same manner as

by Rogers *et al* [19]. The standard Chi-squared value was again obtained using a Chi-squared probability table assuming two degrees of freedom (three laboratories were compared not including the pilot lab) and a significance level of 0.05. The results of the Chi-squared check are shown in table 4.

The bilateral DoE between labs is evaluated and results are reported in table 5. Given that for every comparison the DoE is less than the uncertainty of the DoE, each lab is in good agreement. Here DoE and its uncertainty are reported as relative values.

6. Discussion and conclusion

The comparison of each input condition yielded good agreement across all labs, indicated by very low DoE and expanded uncertainty of the DoE. We observe an average DoE of 0.034% and an associated average uncertainty of 0.35%. Since some of the labs measure with an open-beam configuration and others with a fiber-coupled configuration, this illustrates that the trap detector geometry has high equivalence between differing input beam conditions, making the detectors suitable for a variety of measurement configurations. Additionally, comparison and agreement of all eight traps illustrated consistency in their design, construction and operation. This opens opportunities to lower calibration uncertainties in single photon calibration systems for longer wavelengths. The lower shunt resistance of the large IGA diodes used in this work (compared to Si diodes in [7]) does result in noisy measurements in the pW-regime. This resistance in conjunction with the bias current creates increased noise and drift based on the properties of real operational amplifiers (which are subject to non-zero bias current and non-zero offset voltage). Moving forward, the improvement of current amplifier circuits and potential addition of a voltage reference may reduce noise in low-power measurements. More suitably, development of a trap geometry with smaller diodes and higher sensitivity (and

higher shunt resistance) may allow even lower-power accurate results, provided a similar, scaled geometry is used [20].

ORCID iDs

Kyle Rogers  0000-0003-2470-5286

Jeanne Houston  0000-0002-7597-4649

Matthew Spidell  0000-0002-5513-8520

Padraic Aither  0009-0006-2773-2414

John Lehman  0000-0003-4729-7123

References

- [1] Rahmouni A *et al* 2024 100-km entanglement distribution with coexisting quantum and classical signals in a single fiber *J. Opt. Commun. Netw.* **16** 781–7
- [2] Gerrits T, Migdall A, Bienfang J, Lehman J H, Nam S W, Splett J, Vayshenker I and Wang J 2020 Calibration of free space and fiber-coupled single-photon detectors *Metrologia* **57** 015002
- [3] Vayshenker I, Li X, Livigni D, Scott T and Cromer C 2000 *Optical Fiber Power Meter Calibrations at NIST (Special Publication (NIST SP))* vol NIST SP 250–54 (Department of Commerce, National Institute of Standards and Technology) p 48
- [4] Houston J M and Rice J P 2006 NIST reference cryogenic radiometer designed for versatile performance *Metrologia* **43** S31
- [5] Gallawa R L and Li X 1987 Calibration of optical fiber power meters: the effect of connectors *Appl. Opt.* **26** 1170–4
- [6] Lehman J H and Li X 1999 A transfer standard for optical fiber power metrology *Appl. Opt.* **38** 7164–6
- [7] Lehman J H and Cromer C L 2002 Optical trap detector for calibration of optical fiber powermeters: coupling efficiency *Appl. Opt.* **41** 6531–6
- [8] Fox N P and Martin J E 1990 Comparison of two cryogenic radiometers by determining the absolute spectral responsivity of silicon photodiodes with an uncertainty of 0.02% *Appl. Opt.* **29** 4686–93
- [9] Lehman J, Yung C, Tomlin N, Conklin D and Stephens M 2018 Carbon nanotube-based black coatings *Appl. Phys. Rev.* **5** 011103
- [10] Houston J, Zarobila C J and Yoon H W 2022 Achievement of 0.005% combined transfer uncertainties in the NIST detector calibration facility *Metrologia* **59** 025001
- [11] Buckley S M, Stephens M and Lehman J H 2022 Single photon detectors and metrology *ECS Trans.* **109** 6
- [12] Vayshenker I, Yang S, Li X, Scott T and Cromer C 2000 *Optical Fiber Power Meter Nonlinearity Calibrations at NIST NIST SP 250-56* (Department of Commerce, National Institute of Standards and Technology, Special Publication (NIST SP))
- [13] Vaskuri A K, Stephens M S, Tomlin N A, Spidell M T, Yung C S, Walowitz A J, Straatsma C, Harber D and Lehman J H 2021 High-accuracy room temperature planar absolute radiometer based on vertically aligned carbon nanotubes *Opt. Express* **29** 22533–52
- [14] Niebauer T M, Faller J E, Godwin H M, Hall J L and Barger R L 1988 Frequency stability measurements on polarization-stabilized He–Ne lasers *Appl. Opt.* **27** 1285–9
- [15] Phelan R J and Cook A R 1973 Electrically calibrated pyroelectric optical-radiation detector *Appl. Opt.* **12** 2494–500
- [16] Tomlin N A *et al* 2020 Overview of microfabricated bolometers with vertically aligned carbon nanotube absorbers *AIP Adv.* **10** 055010
- [17] White M, Ruiz Z, Yung C, Vayshenker I, Tomlin N, Stephens M and Lehman J 2018 Cryogenic primary standard for optical fibre power measurement *Metrologia* **55** 706–15
- [18] CCPR Working Group on Key Comparisons 2013 Guidelines for CCPR key comparison report preparation BIPM (available at: <https://bipm.org/utis/common/pdf/CC/CCPR/CCPR-G2.pdf>)
- [19] Rogers K, Williams P, Pastuschek M, Lecher H, Küick S, Lopez M and Lehman J 2024 Multi-kilowatt cw laser power measurement comparison between national standards *Metrologia* **61** 7
- [20] Rahmouni A, Migdall A, Shaw P-S, Rice J P, Slattery O and Gerrits T 2025 InGaAs trap detector: advancing toward a short-wave infrared standard with 1% uncertainty *Appl. Opt.* **64** 2509–14